Central Lancashire Online Knowledge (CLoK)

Title	Treatment of Nocturnal Enuresis using miniaturised advanced mechatronics with Artificial Intelligence
Type	Article
URL	https://clok.uclan.ac.uk/id/eprint/47661/
DOI	https://doi.org/10.1109/JTEHM.2023.3336889
Date	2024
Citation	Kuru, Kaya, Ansell, Darren, Hughes, Dave, Watkinson, Benjamin Jon, Gaudenzi, Fabrizio, Jones, Martin, Lunardi, David, Caswell, Noreen, Montiel, Adela Rabella et al (2024) Treatment of Nocturnal Enuresis using miniaturised advanced mechatronics with Artificial Intelligence. IEEE Journal of Translational Engineering in Health and Medicine, 12. pp. 204-214.
Creators	Kuru, Kaya, Ansell, Darren, Hughes, Dave, Watkinson, Benjamin Jon, Gaudenzi, Fabrizio, Jones, Martin, Lunardi, David, Caswell, Noreen, Montiel, Adela Rabella, Leather, Peter, Irvingr, Daniel, Bennett, Kina, McKenzie, Corrin, Sugden, Paula, Davies, Carl and DeGoede, Christian

It is advisable to refer to the publisher's version if you intend to cite from the work.
https://doi.org/10.1109/JTEHM.2023.3336889

For information about Research at UCLan please go to http://www.uclan.ac.uk/research/

Treatment of Nocturnal Enuresis Using Miniaturised Smart Mechatronics With Artificial Intelligence

KAYA KURU [1], DARREN ANSELL [1], DAVE HUGHES [2], BENJAMIN JON WATKINSON[1],
FABRIZIO GAUDENZI[2], MARTIN JONES[1], DAVID LUNARDI[2], NOREEN CASWELL[3],
ADELA RABELLA MONTIEL[2], PETER LEATHER[4], DANIEL IRVING[2], KINA BENNETT[5],
CORRIN MCKENZIE[2], PAULA SUGDEN[5], CARL DAVIES[1], AND CHRISTIAN DEGOEDE[5]

[1]School of Engineering and Computing, University of Central Lancashire, PR1 2HE Preston, U.K.
[2]Novosound Ltd., EH4 2HS Edinburgh, U.K.
[3]School of Psychology, University of Central Lancashire, PR1 2HE Preston, U.K.
[4]Department of IP and Commercialisation, University of Central Lancashire, PR1 2HE Preston, U.K.
[5]Lancashire Teaching Hospitals NHS Foundation Trust, PR2 9HT Preston, U.K.
CORRESPONDING AUTHOR: K. KURU (kkuru@uclan.ac.uk)

ABSTRACT   Our study was designed to develop a customisable, wearable, and comfortable medical device – the so-called "MyPAD" that monitors the fullness of the bladder, triggering an alarm indicating the need to void, in order to prevent badwetting – i.e., treating Nocturnal Enuresis (NE) at the pre-void stage using miniaturised mechatronics with Artificial Intelligence (AI). The developed features include: multiple bespoke ultrasound (US) probes for sensing, a bespoke electronic device housing custom US electronics for signal processing, a bedside alarm box for processing the echoed pulses and generating alarms, and a phantom to mimic the human body. The validation of the system is conducted on the tissue-mimicking phantom and volunteers using Bidirectional Long Short-Term Memory Recurrent Neural Networks (Bi-LSTM-RNN) and Reinforcement Learning (RL). A *Se* value of 99% and a *Sp* value of 99.5% with an overall accuracy rate of 99.3% are observed. The obtained results demonstrate successful empirical evidence for the viability of the device, both in monitoring bladder expansion to determine voiding need and in reinforcing the continuous learning and customisation of the device for bladder control through consecutive uses.

Clinical impact: MyPAD will treat the NE better and efficiently against other techniques currently used (e.g., post-void alarms) and will i) replace those techniques quickly considering sufferers' condition while being treated by other approaches, and ii) enable children to gain control of incontinence over time and consistently have dry nights. Category: Early/Pre-Clinical Research

INDEX TERMS   Nocturnal enuresis, long short-term memory recurrent neural networks (LSTM-RNN), reinforcement learning (RL), wearable medical devices, incontinence.

I. INTRODUCTION

Nocturnal enuresis (NE), also known as nighttime bedwetting, results in the involuntary discharge of urine due to a congenital or neurological defect [1]. Interested readers are referred to our previous studies [1], [2], [3] to find out more detailed information about NE, its prevalence and its negative effects on children and their families as well as the cost analysis. Besides, current post-void alarms, complementary and/or alternative medicine (CAM), medications that have been deemed unsatisfactory, and previous unsuccessful development trials aimed at finding a pre-void solution were analysed in these studies. Successful treatment of NE both changes the lives of those families significantly and impacts children positively with their daily routines and self-esteem [3], [4], [5] by enhancing the quality of life (QoL).
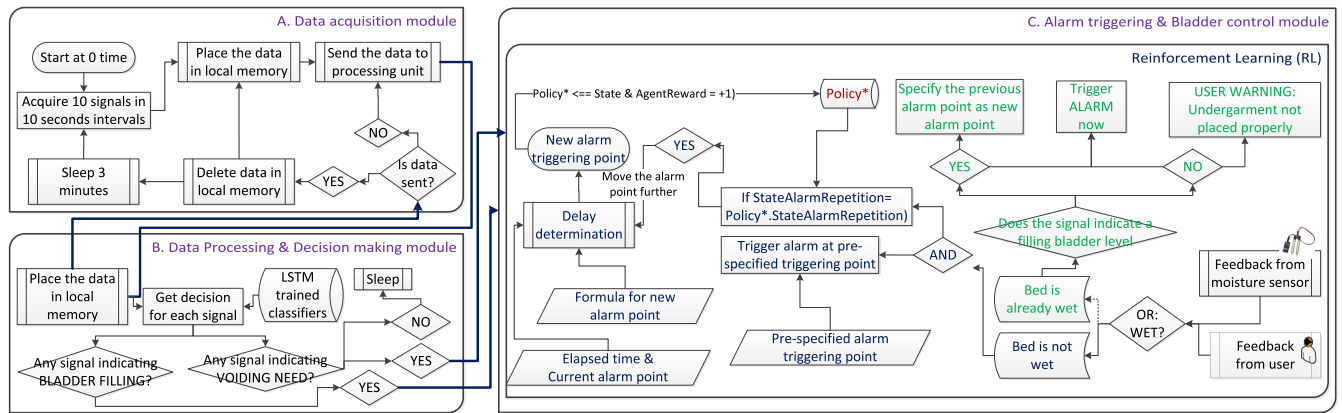
FIGURE 1. Main components and techniques of the modular decision-making methodology.

Smart Mechatronics is a cutting-edge field that is redefining the way medical devices are designed and manufactured. This study has been carried out to develop a miniaturised Advanced Mechatronics System (AMS) that could devise a pre-void alert, minimizing bedwetting, reaching stable dryness through learning bladder control and enhancing QoL for those with NE. AMSs aim to produce high-quality autonomous intelligent products and maintain a competitive edge by improving product performance through effective sensing, self-learning, self-optimisation, self-configuration, self-diagnosis, and precise autonomous decision and actuation [6]. In the framework of this scheme, a wide range of disciplines (e.g., medicine, electronics, ultrasonics, design, data science and Artificial Intelligence (AI)) as well as the relevant community with NE are collaborating to develop a device – the so-called "MyPAD". The main components and techniques of the developed system in this research are outlined in Fig. 1. Following are some of the specific contributions this research makes to clarify its novelty.

1) A bespoke advanced electronic device housing custom ultrasound (US) electronics involving required software for signal processing is developed.
2) A tissue-mimicking phantom is produced, which simulates the human tissue, bladder and its expansion concerning urine-like liquid volume.
3) A cluster of US probes, with low power and low frequency, are designed and built specifically for this application area.
4) The validation of the system is conducted both on the tissue-mimicking phantom and on volunteers using Long Short-Term Memory Recurrent Neural Networks (LSTM-RNN) and Reinforcement Learning (RL) resulting in successful empirical evidence for its viability in monitoring bladder expansion and determining associated voiding need.
5) The developed approach not only triggers a pre-void alarm, but also, aims to help the child i) control his/her bladder with consecutive uses of the MyPAD by modelling the dynamic and nonlinear behaviours of the

bladder and ii) live a normal life without using any device over time.
6) The development of the miniaturised version of the system is still ongoing to enhance its ergonomic use.

The remaining of this research is organised as follows. The proposed system is revealed in Section II. The experimental design is delineated in Section III and the results are presented in Section IV. Discussions are provided in Section V. Finally, Section VI concludes with key findings.

II. METHODOLOGY

A. BACKGROUND

Developing an effective and comfortable device that uses artificial intelligence (AI) techniques to learn and evaluate the bladder, surrounding tissues, and urine intelligently by harbouring customisable abilities for children with various body morphologies is an urgent need to determine imminent voiding needs and provide pre-void alerts accordingly, allowing the child to void with dignity [1]. This device should help the child control his/her bladder with consecutive uses of the device and live a normal life without using any device or medication. Readers are referred to [1] and [2] for the feasibility of such a system and they are referred to [7] for the related patents generated by us in several large countries and regions, namely, Canada (CA2993156A1 (2017)), Europa (EP3328279B1 (2020); EP3834726A3 (2021)), Japan (JP6847943B2 (2021)), China (CN114521896A (2022)) and USA (US11482327B2 (2022)).

Before exploring the particular techniques, approaches, and modules (Fig. 1) in this study in detail, we would like to summarise the particular improvements regarding the previous studies in the following subsections to be able to highlight the main points and glean the novel aspects better in this study.

1) PHANTOM

The phantom established in our previous phases of the project using the chicken tissues could not be used effectively because of its ephemeral characteristics [2] and in this study,

a reusable advanced phantom that mimics the human body, in particular, the bladder, its surrounding tissues, and urine is established, which is described in Section II-B.

2) US TRANSDUCERS

Readers are referred to the supplements of our study in [1] for the detailed analysis of the dynamics of the bladder regarding US beams and the sensors we utilised in our previous phases of the project. PZT (Lead-Zirconate-Titanate), more specifically piezoceramic US transducers are developed in this study because of their response/sensitivity and performance for this particular study on the bladder. The electrodes are placed on the flat surface of the sensing element. The design and development of the cluster probes specific to the subject area are explained in detail in Section II-C.

3) ELECTRONICS HARDWARE

A bespoke advanced electronic device[1] housing custom US electronics, involving required software for signal processing, was developed in our previous study [2]. A miniaturised version of this system (Ex: Figs. 9, 10, 11) is still ongoing to enhance its ergonomy and provide children with a more comfortable wearable bladder monitoring device, which is explained in Section II-D. The techniques in our previous papers have been improved by considering further tests based on the miniaturisation design of the system, which is elaborated in the following section.

4) SOFTWARE/APPLICATION/INTERFACE

We utilised ML techniques, more specifically ensemble techniques (i.e., bagging, boosting) and functions (i.e., Sequential Minimal Optimisation (SMO) and Linear Regression (LR)) to train the datasets collected from the volunteers based on a set of signal features and classify the bladder status in our previous studies [1], [2]. 3/4 full voiding-need triggering point sensitivity (Se) and specificity (Sp) values were 0.89 and 0.93, respectively. Based on the Se value of 0.89, 11 alarms out of 100 might be false alarms causing sleep interruption. Based on the Sp value of 0.93, 7 out of 100 times no alarm sounds when the child should have been woken up, resulting in a wet bed. It was determined that the AI techniques need improvement in order not to cause any predicament for the children and their families as discussed in [1]. In this sense, in this study, we employ LSTM-RNN, a type of RNN to reveal the patterns in acquired signals and to obtain better success rates, which is explained in Section II-D.2 in detail. Furthermore, alarm triggering points regarding the voiding need differ slightly from one child to another and this point should be adjusted and customised concerning the particular characteristics of the child to produce a successful wearable pre-void alarm device that does not require specific training for every child. With this in mind, a new RL technique is developed both to be able to customise the device

autonomously and to help children with NE control their bladder with consecutive uses of the device to live a normal life as their peers. The particular implementation of the novel RL technique is revealed in Section II-D.3. We would like to explain the general aspects of LSTM-RNN here involving the reason why it fits the particular characteristics of the datasets acquired by the sensors in this study. Following the unveiling of LSTM-RNN, the merits of the RL techniques in the customisation of applications in highly dynamic environments, along with their general principles, are pointed out.

a: LONG SHORT-TERM MEMORY RECURRENT NEURAL NETWORKS (LSTM-RNN)

Within a highly connected multi- and hidden-layered network design, a bio/neurons-inspired Artificial Neural Network (ANN) mimics certain functional processing capabilities of the human brain by learning from examples using the connection power of neurons (i.e., weights as the neuron input and basic means of long term memory), particular activation functions, and by reorganising itself from this learning experience in tuning the connection weights through iterations with the backpropagation technique based on output errors and gradual learning. Recently, ANN has been employed successfully with higher accuracy rates in many applications within various disciplines from aerospace to medicine even though it requires both many samples for training and longer processing time compared to feature-based ML approaches. ANN models can extract features on their own different from the feature-based ML techniques through an iterative learning process. ANN can be categorised as Feed-forward Neural Networks (FFNN) and RNN. With FFNN, information is always fed forward, never fed back during learning iterations whereas, with biologically more realistic RNN, feedback loops are possible at any sub-steps of a learning iteration in training cycles. Technically speaking, with FFNN, no links are allowed between the hidden nodes in the same hidden layer while proceeding from the input layer to connected hidden layers and then to the output. RNN is mainly used to describe the temporal dynamic behaviours of time-sequential data [8] where the traditional neural network cannot deal with this kind of problem well because of its limited network design structure [9]. RNN has been proven to yield high performance in classifying time-series sequences for many applications even though it requires a longer computation time for training when compared to FFFN. FFNN with a fixed time window size cannot solve time-series tasks [10] both short- and long-term relevant and hence, we employ LSTM-RNN for determining bladder status with high accuracy rates.

As a kind of RNN and against the regular RNN suffering, vanishing and exploding gradients, LSTM-RNN was first introduced by Hochreiter et al. [11] in 1997. Since then, it has been improved with its newer versions to solve various learning problems for a wide range of engineering applications, in particular, long-term learning dependence problems. LSTM-RNN can memorise long-term dependencies

---

[1] The tissue-mimicking phantom and US electronic device involving the transducers have been developed in the Novosound laboratories.

between consecutive time steps of a sequence [12] using three gates network structure as an inherent memory storing the past information, namely, input, forget and output, by which the information at the cell state used for maintaining long-term information in the hidden layer can be updated selectively using a "receive" and "delete" dynamic process within LSTN-RNN. Furthermore, Bidirectional LSTM RNN (Bi-LSTM-RNN) with forward and backward manner introduced by Schuster and Paliwal [13] can observe complete information and establish temporal dependencies from past and future information in each sequence. More explicitly, the single-directional LSTM-RNN can observe the temporal sequence in the forward direction, while Bi-LSTM-RNN observes it in both directions. Each sample of acquired sensor data in this study represents a timing relationship between frequency cycling within a depth up to 15 cm and LSTM-RNN can acquire these timing relationships successfully as emphasised by Shi et al. [14] where the values of the echoed US pulses before and after any point in our case are not independent, rather, they are strongly related to each other in representing the dynamic status of the bladder as a whole with respect to the expansion with increasing urine based on the elapsing time. Therefore, Bi-LSTM-RNN in the positive and negative time direction is utilised in this study to obtain the past and future information of the echoed pulses in a depth at a time – the propagation of an emitted signal in media and cycles of pulses acquired in different time intervals. The particular implementation of Bi-LSTM-RNN in this research is explained in Section II-D.2.

b: REINFORCEMENT LEARNING (RL)

Without requiring prior datasets/instances for training, RL can be simply described as the science of automated learning by interacting with the highly dynamic environment for exploring and exploiting by using i) model-based methods (e.g., Markov Decision Process (MDP)) or ii) model-free methods with trial-and-error learners in a greedy behaviour to achieve the desired goal – the targeted terminal state. With model-based methods, RL decides on a course of action by considering possible future situations before they are actually experienced, primarily with offline mechanisms with mapping from states to action whereas, with model-free methods, RL behaves with instant trials and observed sub-rewards on sub-states using error learners with online active learning mechanisms. Within this context, RL is highly useful where there are no prior datasets or the environment is changing dynamically and it may not be feasible to train the system using a data set with no patterns, which requires self-learning with interactions with the environment [15]. It maps situations to actions to maximise a numerical reward signal by discovering which actions yield the most reward by trying them [16]. Interested readers are referred to [16] and [17] for more information about RL and its implementation. The particular implementation of RL in our study is explained in Section II-D.3 for customising the device and helping children with NE control their bladder over time.
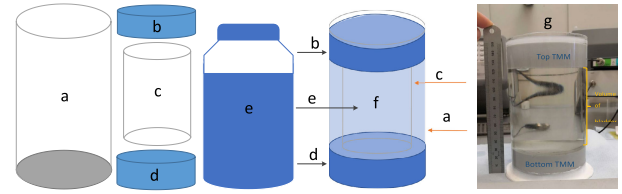

FIGURE 2. Components of the phantom: a) outer perspex cylinder; b) TMM 1 (top) (2.5 cm thick); c) 8 inner perspex cylinders in different heights (1-8 cm) corresponding to the expansion of the bladder from empty to full; d) TMM 2 (bottom) (3 cm thick); e) TMM preservation fluid; f) whole phantom design: container with TMM 1 (top), TMM 2 (bottom), inner perspex cylinder and TMM preservation fluid between these two layers; g) real phantom.

B. PHANTOM DESIGN AND DEVELOPMENT

A tissue-mimicking phantom has been built as illustrated in Fig. 2 to both simulate the human tissue, bladder and its expansion with respect to the changing amount of urine-like liquid and test the efficacy of the developed PZT ultrasonic transducers (Section II-C) and mechatronics (Section II-D.1) as well as the application (Sections II-D.2 and II-D.3). The phantom is composed of a container and two tissue-mimicking materials (TMMs). TMM is designed for the acoustic and thermal characterisation of high-intensity focused US (HIFU) devices to mimic the human body. It is produced from a material that encompasses similar acoustic characteristics of the human's soft tissue. Currently, there is a variety of TMMs used both commercially and within laboratories. Normally, TMM is manufactured under the International Electrotechnical Commission (IEC) 2001 "Ultrasonics - flow measurement systems - flow test objects" [18]. For this project, the acoustical features of these TMMs are designed to match with US parameters and features suggested by the IEC. More information can be found under the term "IEC agar-TMM" The basic ingredients of TMM are water, glycerol, agar, aluminium oxide powder (in two different particle sizes), silicon carbide and benzalkonium chloride which acts as an antibacterial agent.

With regards to the acoustic properties, TMM has been manufactured to have 1544 ± 3.5 m/s, the speed of sound, and attenuation of 0.5 ± 0.05 dB/cm at room temperature, which increases with frequency [19]. A particular TMM preservation fluid is needed to prevent TMM from drying and glycerol leaching which occurs when the TMM is simply immersed in water; Drying and glycerol leaching cause changes in the acoustic properties of the TMM [19]. The acoustic characterisation of the TMM preservation fluid was performed by the National Institute of Physics (NPL, Teddington, UK) [19]. The speed of sound was measured as 1538.15 ± 0.22 m/s with an attenuation of $\alpha([dB\ cm]) = 0.00309f^2 - 0.004996f$ as a function of frequency, over the frequency ranging between 1 - 60 MHz. The ingredients of the TMM preservation fluid [20] are summarised in Table 1.

C. MULTIPLE SENSOR DESIGN AND DEVELOPMENT

Detection of desired echoed pulses may not be possible using one receiver because of the reflection and the refraction

TABLE 1. Compounds of TMM preservation liquid.

Ingredients	Volume (ml)
99% Glycerol	143.9
10% Benzalkonium Chloride	58.71
Degassed deionized water	1000

of emitted incident beams and the dynamics of the bladder. The reflection at the interface of two media is calculated using the formula, R = (Z1-Z2/Z1+Z2) [21] where Z1 represents the impedance value of the proximal side of the interface and Z2 represent the impedance value of the distal side. No refraction occurs at the interface if the beam is perpendicular no matter what the sound speed difference is between the two materials. On the other hand, the refraction occurs based on Snell's law, $sinQ_t/sinQ_i = c_2/c_1$ [21] where c_1 and c_2 indicate the propagation speed of the US beams within the first media and second media respectively. Therefore, 4 receiver transducers and 1 transmitter transducer are incorporated into the study and in this way, we intend to acquire desired echoed pulses using at least one sensor based on the US refraction and reflection laws.[2] The design and development of the cluster probes to be connected to the electronics are depicted in Fig 3.
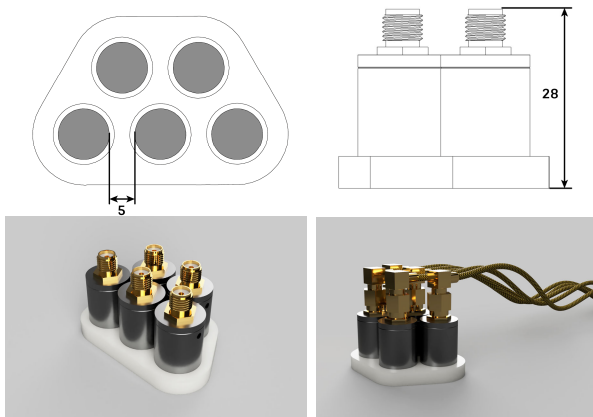

FIGURE 3. Cluster design of miniaturised probes with 5 mm apart.

Various particular PZT (Lead-Zirconate-Titanate), more specifically piezoceramic US transducers have been developed because of their large response/sensitivity and performance. The features of the transmitter and the receivers are explained in Table 2. An example of the data acquisition interface is provided in Fig. 4 using the probes which have their housing displayed in Fig. 5 d.

D. COMPONENTS OF ELECTRONICS AND SOFTWARE IMPLEMENTATION
1) ULTRASOUND ELECTRONICS
The components of the hardware involving their connection to each other to collect data samples are shown in Fig. 5. The functions of these components as well as their properties are

[2]The physics of US on the human body, particularly bladder and urine was explored in our previous study [1] in detail.

explained in Table 2. 19,879 data points representing 15 cm of the propagation depth of US beams throughout the human body are acquired per channel, i.e., a receiver that makes use of these electronics. The pulses are sampled at a frequency sample of 100 Hz. An example of data points acquired at a time from four channels involving their A-mode presentation is provided in Fig. 4.
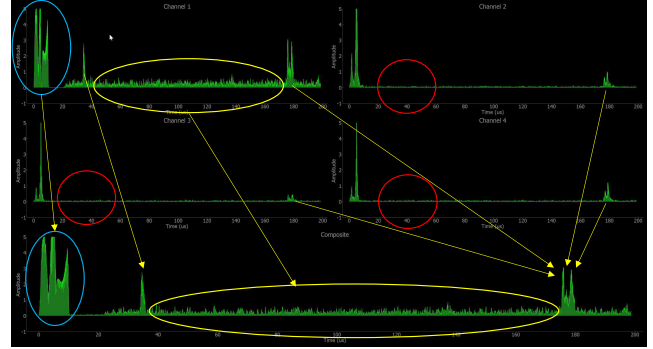

FIGURE 4. Pulse acquisition interface: Pulses with 4 receivers in their dedicated channels and their composite outcome at the bottom. The first amplitudes in the frames correspond to the echoed pulse coming from the anterior wall whereas the second amplitudes correspond to the pulses from the posterior wall of the bladder. The red circles indicate the places where no echoed pulses are detected from the anterior wall because of the reflection and refraction angles of the emitted US beams from the transmitter. The amplitudes in the yellow ovals indicate the noise caused by the high signal-to-noise ratio.
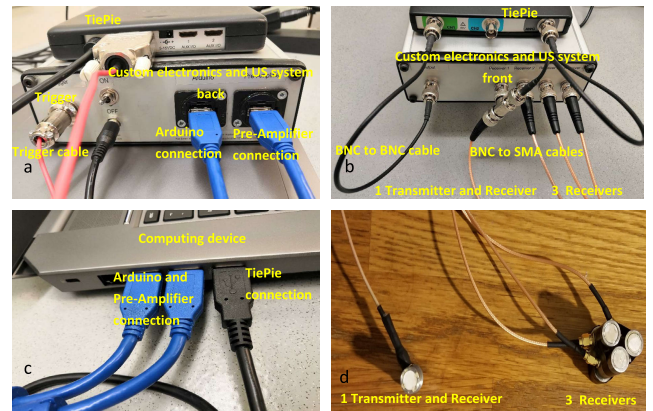

FIGURE 5. Components of the electronics and their connection.

2) SOFTWARE IMPLEMENTATION: DEVELOPMENT OF LONG SHORT-TERM MEMORY RNN (LSTM-RNN)
LSTM-RNN is employed to classify the US data acquired from the phantom, bladder and its surrounding tissue over a period of time in different filling levels. There are five types of data representing the bladder status, namely, i) empty bladder, ii) quarter bladder, iii) half bladder, iv) three-quarters bladder, and v) full bladder. The voiding need usually starts at the 3/4 bladder level where the bladder wall gets thinner as the urine fills the bladder and hence, pressure on nerves is expected to increase [1], [2]. Therefore, the system is

TABLE 2. Features of the elements presented in Fig. 5.

Components	Properties	Functions
Custom electronics and US system	Arduino, 4 channel pre-amplifier, US system	Short-term memory; Gain in the receive stage: currently set to 40 dB; sampling frequency: current value 200MSa/s; averaging 4; chirp parameters including start/stop frequency (current value 0.55-8MHz), duration (8us) and Tukey window
TiePie	Differential / single-ended switchable inputs with SafeGround protection; 1 GS/s 14-bit quad differential channel high-resolution PC oscilloscope; point-by-point arbitrary waveforms with exceptionally low jitter and high fidelity; 7.45 Hz resolution bandwidth and 140 dB dynamic range	Quick setup for every type of measurement; continuous data logging; SafeGround to protect the measuring object; SureConnect to make sure the oscilloscope probe is connected; CMI to couple more instruments to one multi channel instrument, high-resolution and the lowest noise; generate pulses
Transmitter	Flexible frequency generation PZT transducer with a center frequency of 10MHz with a wideband enough to be used with a chirp sweeping from 5MHz to 15MHz.	Transmit the pulses in various frequencies.
Receivers	PZT sensors with a resonant center frequency of the receiver probes is 4.3MHz with a bandwidth of ranging from 2MHz to 8MHz.	Receive the echoed pulses.
BNC to SMA cables	BNC: British Naval Connector or Bayonet Nut Connector,a type of connector used with coaxial cables; SMA: Signal magnitude area, a measure of the magnitude of a varying quantity	Establishment of the connection between the sensors and the US system (the connection between the EP system and the D185 multi-pulse cortical stimulator from digitimer)
BNC to BNC cable	BNC: British Naval Connector or Bayonet Nut Connector, a type of connector used with coaxial cables	Establishment of the connection between the TiePie and the US system (the connection between the EP system and the D185 multipulse Cortical Stimulator from digitimer)
Trigger cable	Stimulator	Generation of pulse trigger
USB cables	USB3	Establishment of the connection between the 1) Arduino and the USB hub, 2) pre-amplifier and the hub
Power supply	AC Adapter; input:100-240 V; output: 12V	Provide the required currency for custom electronics and US system

expected to classify 3/4 bladder and full bladder in one group as "Alarm" and the rest prior to the 3/4 bladder level in another group as "No-Alarm" (Fig. 7). In this way, the system can trigger an alarm to wake up the child when a voiding need is detected – i.e., an acquired data is classified as "Alarm" in a binary classification by differentiating acquired echoed pulses that fit the features (e.g., characteristics of the amplitudes, distances between amplitudes, distances of amplitudes from the sensors) in "Alarm" class from the pulses indicating the features in "No-Alarm" class.

In our research, a single-layer Bi-LSTM-RNN with fully connected layers and 100 hidden units is established to distinguish "Alarm" pulses from "No-Alarm" pulses using one-dimensional input and binary output. The hidden units in the last hidden state from the forward direction and in the first hidden state from the backward direction are interconnected to feed the output layer with a softmax layer. The outputs of the softmax layer maintain the scores for the 'Alarm'' and "No-Alarm" classes. The selected parameters that suit the computing device and the distribution and characteristics of the datasets for the training phase of Bi-LSTM-RNN are presented in Table 3. These parameters have been determined after several trials to obtain the best possible accuracy rate. For instance, the epoch parameter with 30 results in a *Se* value of 98.6 and a *Sp* value of 97.5; the epoch parameter with 50 results in a *Se* value of 98.7 and a *Sp* value of 97.1 with a problem of overfitting, which are less than the values obtained by the epoch with 40 (Table 7). With a problem of overfitting, training using epoch with 50 shows that the accuracy is not improving and it is not converging to a desired solution with the oscillated upward and downward values without a specific direction. The module, namely, "B. Data processing & Decision making" as outlined in Fig. 1 functions based on the classifiers established by Bi-LSTM-RNN after the sensor data is acquired as described in the module, "A. Data acquisition".

TABLE 3. Main parameters used in Bi-LSTM-RNN.

Parameters	Values	Explanation
Layers	- sequenceInputLayer = 1 - bilstmLayer =100, - OutputMode = last - fullyConnectedLayer(2) - softmaxLayer - classificationLayer	- sequence input with 1 dimensions - bidirectional with 100 hidden features - output the last element of the sequence - 2 fully connected layer, two classes - softmax layer - classification layer
Epochs	- MaxEpochs = 40	- 40 times over the training dataset
Batch size	- MiniBatchSize = 50	- 50 Iteration (training pulses) per epoch
Learning rate	- InitialLearnRate = 0.01	- accelerate the learning process
Sequence length	- SequenceLength = 1000	-split the input pulse into smaller sizes, -easier processing by computing device
Curve threshold	- GradientThreshold = 1	- prevent the curve from getting too large
Environment	- ExecutionEnvironment = GPU	- use GPU for processing
Process monitoring	- plots = training-progress	- show the training iterations as processed
Progress	- Verbose = true	- show the data output

3) SOFTWARE IMPLEMENTATION: DEVELOPMENT OF REINFORCEMENT LEARNING

The RL technique developed in the methodology is used to address various uncertainties within instant dynamic calculations, leading to a goal state or a terminal state through a sequence of actions. Using the deterministic policy, this particular technique entitled "Reinforcing stimulus for NE (RstiNE)" is outlined in the dedicated section titled "C. Alarm triggering & Bladder control module" in Fig. 1 and is also presented within the pseudo-code in Algorithm 1. RstiNE using a model-free method with action (exploration) and selection (exploitation) policy (π) aims to help the child control his/her bladder with consecutive uses of the device in order to live a normal life without using any device. Therefore, the alarm triggering point (i.e., the current state of the environment) is moved further gradually (i.e., 0.5 mm) from 3/4 bladder (i.e., ≈6 cm [2]) up to full bladder (i.e., ≈8 cm [2]) as the child learns the controlling of the previous alarm points. More explicitly, the current point is aimed to be moved 0.5 mm further (i.e., one step

Algorithm 1 Reinforcement Learning: C. Alarm triggering & Bladder control module (Fig. 1 C)

Data: System input: CurrentAlarmPoint & AlarmRepetition & ElapsedTime & USSensorBladderFILLING &USSensingTime & MoistureSensingTime) & UserSensingTime & GOAL & *Policy**

Data: Instant input: UserWET & MoistureSensorWET & USSensorALARM & UserAlarmSTOP & GOAL

Result: triggerAlarm & NewAlarmTriggeringPoint & DelayTime

1 =>User starts the system after placing the undergarment as instructed;
2 =>Reading from bladder started;
3 **while** *NOT UserAlarmSTOP* **do**
4   =>Alarm and learn where the bed is wet;
5   **if** *NOT(UserWET== Null && USSensorALARM==False && MoistureSensorWET==False)* **then**
6   =>The system works as desired;
7   **if** *USSensorALARM==True && MoistureSensorWET==False && UserWET==False* **then**
8   triggerALARM(); AlarmRepetition = +1;
9   **if** *StateAlarmRepetition== Policy*.StateAlarmRepetition && NOT (GOAL == FullBladder)* **then**
10   =>Alarm point incresed by 0.5 mm up to 20 mm;
11   =>Alarm time calculated w.r.t. new alarm point(Table 4 or Table. 6);
12   AlarmRepetition=0; [NewAlarmTriggeringPoint, DelayTime, GOAL] = alarmPointFurther(CurrentAlarmPoint,ElapsedTime);
13   *Policy** <== (State & AgentReward=+1);
14   EXIT();
15   =>The system not working as desired;
16   **else if** *USSensorALARM==False && (MoistureSensorWET==True || UserWET==True)* **then**
17   triggerALARM();
18   =>Check if undergarment placed properly;
19   **if** *USSensorBladderFILLING==True* **then**
20   =>Alarm point reduced by 0.5 mm;
21   [NewAlarmTriggeringPoint] = alarmPointBack(CurrentAlarmPoint);
22   *Policy** <== (State & AgentReward=-1);
23   EXIT();
24   **else**
25   voiceAlarm"Please place the undergarment as instructed";
26   EXIT();
27   **end**
28   **else if** *USSensorALARM==True && (MoistureSensorWET==True||UserWET==True)* **then**
29   triggerALARM();
30   =>If USSensingTime smaller than other two sensing inputs;
31   **if** *(USSensingTime<MoistureSensingTime) && (USSensingTime<UserSensingTime)* **then**
32   Goto Line 8;
33   **else**
34   =>Alarm point reduced by 0.5 mm;
35   [NewAlarmTriggeringPoint] = alarmPointBack(CurrentAlarmPoint);
36   *Policy** <== (State & AgentReward = -1);
37   EXIT();
38   **end**
39   **else**
40   voiceAlarm"Exception";
41   **end**
42   **else**
43   SLEEP 3;
44   **end**
45 **end**

---

ahead from the current experience) after the consecutive successes at that point (i.e., $>$ *Policy**.StateAlarmRepetition) based on the reward, R_t (i.e., feedback signal given directly by the environment – from the user, moisture sensor and/or application indicating how well the system is doing at the current state as a teaching agent: with the aim of maximising the expected rewards – value function ($V^* = \sum_{n=1}^{t} f(s_n, a_n, r_n)$) in long-term policy making, learning agent gets rewarded at the states either for successes by 1
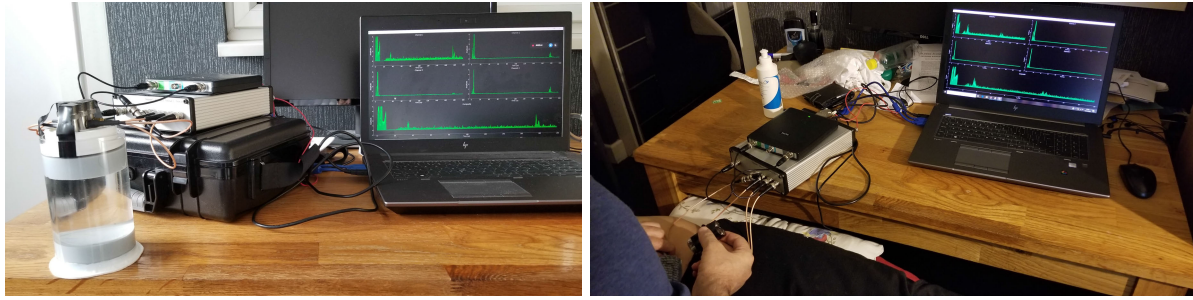
TABLE 4. Formula for determining the delay time based on the filling time of the 3/4 bladder status.

$DelayTime(min) = (Elapsed3Q(min)*$ $(CurrentAlarmPoint(mm) + 0.5(mm)))/60(mm);$
$if\ CurrentAlarmPoint < 20 \wedge InitialAlarmPoint = 3/4;$
where Elapsed3Q = start time (0 min) - end time (3/4 bladder), CurrentAlarmPoint indicates the previous alarm point in mm determined by this formula after 60 mm that indicates the 3/4 full bladder level in children [2] and 0.5 mm corresponds to the amount of moving the alarm triggering point further. Conversely, the current alarm point is moved back when the child wets the bed with the current point to help reinforce the learning through the exploring and exploitation steps.

*Policy** $<==$ (State & AgentReward= +1) or for failures by -1 (*Policy** $<==$ (State & AgentReward=−1))). Moving the alarm point further is realised by a delay time calculated based on the initial alarm point (i.e., voiding need (3/4 bladder)) determined by the trained Bi-LSTM-RNN classifier as explained in Section II-D.2. The formula for determining the delay time based on the filling time of the 3/4 bladder status (i.e., the elapsed time until the 3/4 filling level) to move the current alarm point forward by 0.5 mm is given in Table 4. In this way, irregular rapid changes in the bladder resulted from various conditions (e.g., i) filling time of the bladder based on the liquid consumed, ii) contraction of the bladder wall based on the bladder expansion for triggering a nerve stimulus, and ii) particular characteristics of the child) are aimed to be mitigated by referencing the most recent observed dynamic information. By maximising the cumulative reward with a convenient selection of actions/transitions (i.e., state-action-reward $- s_n, a_n, r_n, s_{n+1} \ldots$), the RL agent behaves greedily to achieve the final goal (i.e., the terminal state or final reward) that is reaching the full bladder status without wetting the bed and voiding in a dignified manner in that state with tuning the settings with most appropriate adjustments by updating the current state of the action every time.

The initial triggering alarm point might be earlier than the 3/4 bladder filling level for several children, most probably between 1/2 bladder and 3/4 bladder and needs to be customised regarding the particular characteristics of the child. In this case, RstiNE takes the 1/2 bladder level as a reference point to specify the initial starting alarm point and does the calculations mentioned above accordingly. However, this time, the system is not taking the 1/2 bladder classifier as a starting point instead of the 3/4 bladder classifier, because, taking a point well behind the required voiding point would hinder the learning at the start of the use of the device. The formula to calculate the initial starting alarm point in mm based on the 1/2 bladder level and bedwetting time is given in Table 5.

TABLE 5. Formula to calculate the initial starting alarm point in mm based on the 1/2 bladder level and bedwetting time.

$InitialAlarmPoint(mm) = ((40(mm)X(ElapsedWet(min)-$ $ElapsedHalf(min)))/ElapsedHalf(min)) - 0.5(mm);$
where InitialAlarmPoint is a point that indicates 0.5 mm back of the bedwetting moment and a distance further away from the 1/2 bladder level; ElapsedWet indicates the time when the bed gets wet from the start time; ElapsedHalf corresponds to the time taken to get the 1/2 bladder filling level determined by the Bi-LSTM-RNN classifiers.

FIGURE 6. Data collection from the phantom (full bladder) (left) and the volunteer (3/4 full bladder) (right).
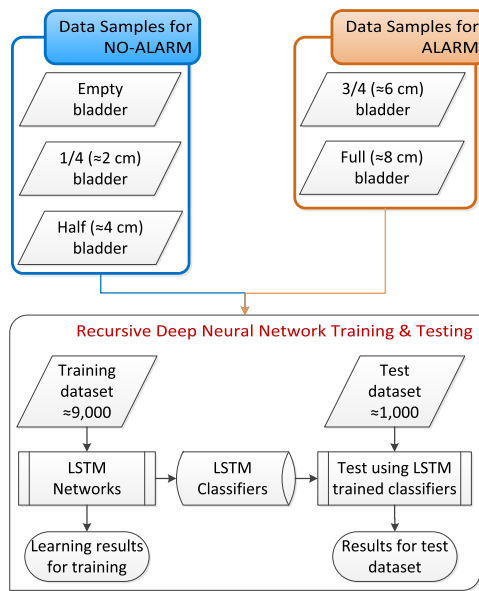

FIGURE 7. Phases of data processing.

TABLE 6. Formula to determine the delay time based on the initial starting alarm point and the current alarm point.

$$DelayTime = (ElapsedHalf(min)X(InitialAlarmPoint(mm) + CurrentAlarmPoint(mm) + 0.5(mm)))/(40(mm) + InitialAlarmPoint(mm));$$

$$if\ InitialAlarmPoint + CurrentAlarmPoint < 3/4\ bladder\ level;$$

where ElapsedHalf corresponds to the time taken to reach the 1/2 bladder level; InitialAlarmPoint is the point determined by Table V; CurrentAlarmPoint indicates the previous alarm point in mm determined within this formula.

The linear increase of the moving alarm point (i.e., currently 0.5 mm) might be needed to be gradually reduced using a realistic mapping function with respect to the particular features as the alarm point approaches the full bladder level where the pressure on nerves is supposed to increase as the bladder wall gets thinner. We need to observe this issue as the device is used by a sufficient number of children with NE. On the other hand, the termination point for the RL technique – full bladder is calculated by the delay time in Table 4 where it indicates a ≈2 cm distance from the 3/4 bladder level or in Table 6 where it indicates a ≈4 cm distance from the 1/2 bladder level based on the bedwetting reference point. Alternatively, the full bladder level determined by the

Bi-LSTM-RNN classifiers can be used to specify the termination point for the RL technique. In any case, the termination point determined by these two approaches differently is expected to indicate the same point and we would like to observe this issue with our 14-week test on more volunteers to be able to conclude safely.

III. EXPERIMENTAL DESIGN

A computing device with a GPU (Fig. 6) supported by the Parallel Computing Toolbox of Matlab is used to mitigate the very long training process and computational burden of training in Bi-LSTM-RNN. 10,000 data samples representing different filling levels with different positioning and angles of the probes as shown in Fig 7 have been collected both from the phantom using the inner perspex cylinders (see Fig 2 c) in different heights and 2 volunteers as depicted in Fig 6. Only, the composite data samples on which the distinctive values of the sensor channels (see the top 4 subplots in Fig. 4) regarding their amplitude are projected (see the bottom subplot in Fig. 4 are used to train the network. 9,000 data samples are used for the training process and 1,000 data samples are reserved for the evaluation of the trained network (Fig 7), in other words, to test the accuracy of the network classifiers on the new data samples to be able to observe both their performance on the dataset not involved in the training phase and if the number of the dataset is sufficient in regards to representing the real-world environment by avoiding overfitting. The progress of the training network phase is depicted in Fig 8 along with the main selected parameters.

TABLE 7. Confusion matrix of the classifiers.

		A. Training/Testing Results			B. Evaluation Results		
		Actual Class			Actual Class		
		Alarm	No-Alarm	%	Alarm	No-Alarm	%
Pred	A	4417 (TP)	21 (FP)	99.5 (PPV)	476 (TP)	4 (FP)	99.2 (PPV)
	NA	43 (FN)	4395 (TN)	99.0 (NPV)	14 (FN)	486 (TN)	97.2 (NPV)
	%	99.0 (Se)	99.5 (Sp)	**99.3 (ACC)**	97.1 (Se)	99.2 (Sp)	**98.2 (ACC)**

IV. RESULTS, EVALUATION, AND VALIDATION

Oversampling was employed during the training phase to equalise the two groups to avoid the classification bias that might emerge while detecting the lesser number of "Alarm" events in the larger population of "No-Alarm" events (i.e., 87.3%) (Fig 7). Furthermore, the distribution
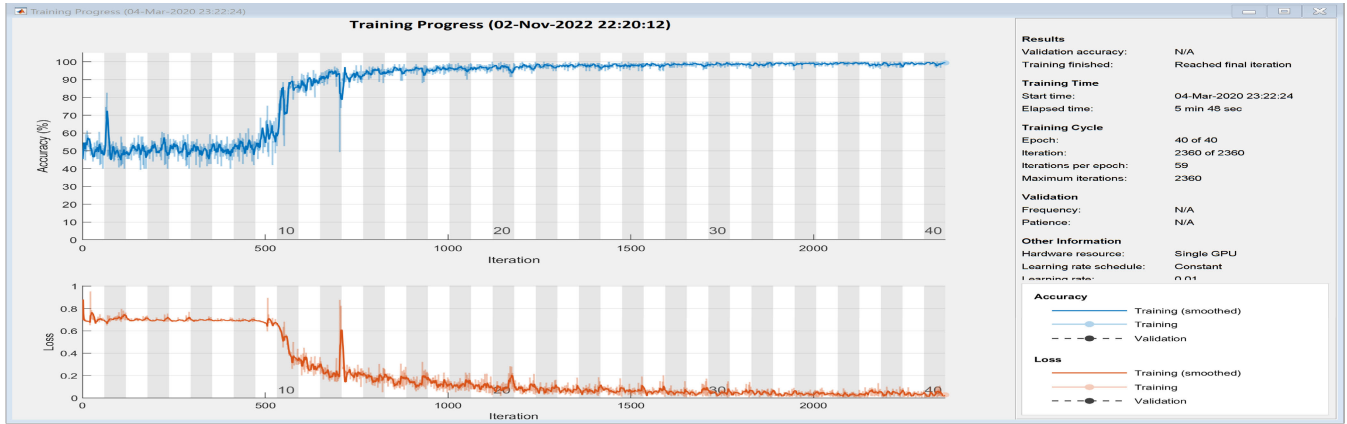
FIGURE 8. Training phase of Bi-LSTM-RNN: The top subplot presents the progress of the training accuracy and the bottom subplot shows the cross-entropy loss on each mini-batch – i.e., the reducing error down to zero if the training progresses successfully.

between "No-Alarm" and "Alarm" signals was evenly balanced in the training and testing sets while selecting batch samples to avoid any possible training bias and to make the outcome resilient. Cross-entropy loss, one that approaches zero (Fig 8 bottom) was used as a loss function while optimizing the classification model of the Bi-LSTM-RNN. The results of the training phase are summarised in Table 7 A. A Se value of 99% and a Sp value of 99.5% with an overall accuracy rate of 99.3% are observed in this process, which seems highly satisfactory. Strictly speaking, 99% of "Alarm" signals are correctly classified as "Alarm" and 99.5% of signals classified as "No-Alarm" are actually "No-Alarm". On the other hand, the trained network classifiers are evaluated on the reserved dataset (i.e., 1,000 data samples) and a Se value of 97.1% and a Sp value of 99.2% with an overall accuracy rate of 98.2% are observed in this process as shown in Table 7 B. Even though these results obtained from the evaluation dataset are high, they, particularly the Se value, are below the values obtained during the training phase (i.e., 99-97.1 $\approx$ 1.9). This difference suggests that the 10,000 data samples do not precisely represent the real-world environment regarding the number of "Alarm" events and should be increased by several thousand to improve the Se to a level that the training phase has in order to avoid any possible overfitting. It is noteworthy to emphasise that Precision (Pr), i.e., Positive Predictive Value – $PPV=Pr = TP / (TP + FP)$ – is 0.995 and 0.992 for the training/testing and evaluation phases (Table 7). These high values demonstrate that the model is highly successful in assigning "Alarm" events to the "Alarm" class. In other terms, the number of false alarms causing sleep interruption is reduced significantly. Having said this, the number of the anticipated "Alarm" will be 1 (or 2 maximum) for a night. This means that 1 out of 160 echoed pulses is supposed to be an "Alarm" for a night where beams are emitted in every 3-minute intervals during the 8 hours of sleep until the child is awoken with an "Alarm". From this perspective, the child is supposed to use the device for a maximum of 14 weeks (i.e., 98 days), which means that

the alarm might be missed for a maximum of 3 days wherein involuntary voiding may occur, but the user is enabled to void with dignity during the remaining 95 days. From the other perspective, the next "Alarm" pulse will definitely be detected as "Alarm" while the Se value is 97.1% before voiding after the first "Alarm" has been missed for 3 minutes. More explicitly, beam emitting time intervals can be adjusted accordingly, i.e., shortened (e.g., from 3 minutes to 1), to capture the next "Alarm" pulse correctly before voiding occurs. However, under these circumstances, the number of FPs will increase leading to sleep interruption regarding the Sp, 99.2%, e.g., 5 times among 480 signals emitted for each minute. In other words, the more signal generation, the more FPs, causing sleep interruptions. In this case, the alarm can be triggered if 2 or 3 consecutive "Alarm" events are observed (i.e., "Alarm" + "Alarm" = "Alarm" or "Alarm" + "No Alarm" = "No Alarm") to avoid sleep interruptions where 5 FPs will be distributed randomly among 480 "No Alarm" events through the random probability distributions – two or more FPs will not be observed in detected consecutive echoed pulses. In this way, it can be concluded that the child will never wet the bed by being awoken by the next two consecutive "Alarm" events if the first one has been skipped by the system, leading to no unintentional sleep interruption. This validates the robustness of the system even though a very small number of FNs ($Se = 97.1\%$) and FPs ($Sp = 99.2\%$) may occur.

V. DISCUSSION
There is increasing evidence that non-invasive pre-void alarm systems can assist the younger demographic suffering from NE in alleviating their problems significantly. The market currently offers post-void alarms that are not considered adequate. Our study was designed to develop a customisable, wearable medical device that generates pre-void alarms using miniaturised mechatronics with Artificial Intelligence (AI). The data samples in the datasets used in this study involve data samples related to the echoed pulses within a

depth of 15 cm propagation of US signals through the body with a sequence of data points, particularly, time pitches of sequence data. These data samples are acquired in regular time intervals. With slightly changing features, they are strictly related to each other as the bladder expands with the filling of urine, which requires a time-series analysis. Therefore, Bi-LSTM-RNN that can manage the sequence and time-series analysis successfully is employed in this study. The results suggest that the Bi-LSTM-RNN-based approach substantially outperforms the feature-based ML techniques (see Section II-A.4 and our previous study [1]) based on the A-mode US signals and the datasets acquired from the human body, primarily from the bladder. Furthermore, with the help of the RL technique – RstiNE (Algorithm 1) built in the study, the system does not need to train itself for each child for customisation. From a technical standpoint, essential sensitive customisation and adjustments per child can be carried out intelligently in an autonomous manner by considering the particular characteristics of the child during the use of the device. More explicitly, the system, with RstiNE, is turned into an intelligent system built upon Bi-LSTM-RNN with pre-trained classifiers. It becomes a perpetual intelligent learning system using RstiNE. The studies on alarm therapy [22], [23], [24], [25] suggest that the child with NE can learn to control his/her bladder using alarms over time. In this sense, the pre-stimulus ability of RstiNE at the desired points of the bladder filling levels customised per child helps children control their bladders by adjusting their behaviours over time yielding to the reduction of the frequency of NE. With self-customisation abilities and increased efficacy, the device can be used without requiring non-trivial and long pre-training phases or manual customisation, which makes the device highly attractive and functional in behaving specifically to the particular needs of the child as desired with no engineers and expert knowledge.
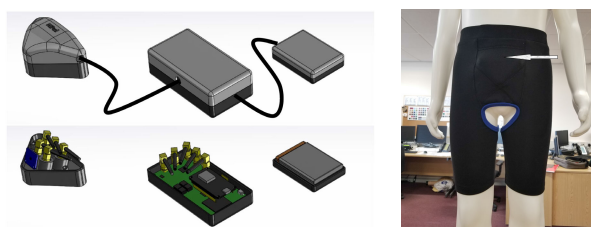

FIGURE 9. Design of the MyPAD with sensors, electronics, and battery and its use with the undergarment on a manikin.

With the crafted miniaturised version of the data acquisition electronics with a size of 110 mm by 80 mm, the device can be easily and comfortably placed in the undergarment as shown in Fig. 9. An example of the early miniaturisation trials of the device is displayed in Fig. 10. The first prototype assembly of the MyPAD device is depicted in Fig 11. International standards such as CE mark, comfort (e.g., more ergonomic geometry, aesthetics, and further miniaturised casing with further miniaturised electronics and sensors), and
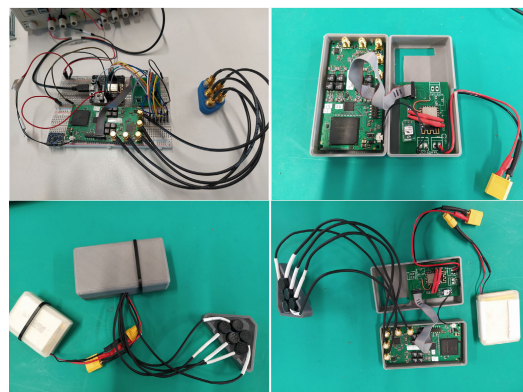

FIGURE 10. Early miniaturisation of the device.

FIGURE 11. First prototype assembly of the device.

safety concerns (e.g., waterproofing, cables, heating of the electronics) will be ensured before long-term use of the device with more volunteers. The developed techniques are aimed to be validated on this device with 10 children that have NE after these standards have been certified. Then, the device is aimed to be inspected with larger groups before mass production for commercialisation. The results of the completed miniaturised device will be published in our next paper after extensive tests and trials with children. The single-to-noise ratio (SNR) is expected to be reduced significantly. It is worth noting that the performance of the LSTM-based method is expected to increase with the high quality of input signals regarding less signal-to-noise ratio. Therefore, new datasets will be collected both from the phantom and more volunteers to train the system using the finalised miniaturised version of the device with less signal-to-noise ratio. Thereafter, the aim is to test the enhanced miniaturised device with the younger demographic suffering from NE for 14 weeks to i) get feedback associated with wearability and treatment of NE, and ii) improve the decision-making ability of Bi-LSTM-RNN concerning various morphology types with more training data collected via the cloud platform. With these tests, we expect to conclude safely if 14 weeks is sufficient for the child to learn how to control his/her bladder using intelligent autonomous monitoring and customisation approaches built in this research.

VI. CONCLUSION
Our study was designed to develop a customisable, wearable medical device that generates pre-void alarms using

miniaturised mechatronics with Artificial Intelligence (AI) to treat NE. In this context, the developed features include: multiple bespoke US probes for sensing, a bespoke electronic device housing custom US electronics for signal processing and a bedside alarm box for processing the acquired signals and generating alarms. With the implemented Bi-LSTM-RNN in the study, we achieve a notable accuracy improvement on the results compared to the results obtained from the state-of-the-art feature-based ML classification techniques in regards to the A-mode-based US datasets acquired from deep within the human body, primarily from the bladder. Moreover, incorporation of the RL technique – RstiNE – proposed in the study into the decision-making phase not only helps customise the device for the particular characteristics of the user, especially finding the specific alarm points of their bladder without needing any prior training, but also, supports users to control their bladder with consecutive uses of the device. The MyPAD device will highlight any differences in terms of bladder fullness, leading to triggering of the alarm and the need to void, for each child with NE, which will be useful for those tasked with treating the condition and for the child it will vastly improve their quality of life. Other potential applications of My-PAD include stroke patients, elderly care (geriatric) settings, urine retention diagnosis, and veterinary science. Furthermore, this study sheds light on studies with similar datasets about how to incorporate ANN and RL into their studies to obtain the best possible results from a clinical transitional perspective.

ACKNOWLEDGMENT

REFERENCES

[1] K. Kuru, D. Ansell, M. Jones, C. De Goede, and P. Leather, "Feasibility study of intelligent autonomous determination of the bladder voiding need to treat bedwetting using ultrasound and smartphone ML techniques," *Med. Biol. Eng. Comput.*, vol. 57, no. 5, pp. 1079–1097, May 2019.

[2] K. Kuru et al., "Intelligent autonomous treatment of bedwetting using non-invasive wearable advanced mechatronics systems and MEMS sensors," *Med. Biol. Eng. Comput.*, vol. 58, no. 5, pp. 943–965, May 2020.

[3] N. Caswell et al., "Patient engagement in medical device design: Refining the essential attributes of a wearable, pre-void, ultrasound alarm for nocturnal enuresis," *Pharmaceutical Med.*, vol. 34, no. 1, pp. 39–48, Feb. 2020.

[4] O. Mowrer and W. Mowrer, "Enuresis: A methods for its study and treatment," *Amer. J. Orthopsychiatry*, vol. 2, no. 4, pp. 259–267, 2005.

[5] B. Hägglöf, O. Andren, E. Bergström, L. Marklund, and M. Wendelius, "Self-esteem in children with nocturnal enuresis and urinary incontinence: Improvement of self-esteem after treatment," *Eur. Urol.*, vol. 33, no. 3, pp. 16–19, 1998.

[6] K. Kuru and H. Yetgin, "Transformation to advanced mechatronics systems within new industrial revolution: A novel framework in automation of everything (AoE)," *IEEE Access*, vol. 7, pp. 41395–41415, 2019.

[7] D. W. Ansell, C. Sanders, P. Leather, K. Kuru, and M. Amina, "Methods and apparatuses for estimating bladder status," Univ. Central Lancashire, Preston, U.K., WO Patent 2017/017 426, 2017. [Online]. Available: https://patentscope.wipo.int/search/en/detail.jsf?docId=WO2017017426

[8] X. Yuan, L. Li, and Y. Wang, "Nonlinear dynamic soft sensor modeling with supervised long short-term memory network," *IEEE Trans. Ind. Informat.*, vol. 16, no. 5, pp. 3168–3176, May 2020.

[9] H.-X. Tian, D.-X. Ren, and K. Li, "A hybrid vibration signal prediction model using autocorrelation local characteristic-scale decomposition and improved long short term memory," *IEEE Access*, vol. 7, pp. 60995–61007, 2019.

[10] F. Gers, D. Eck, and J. Schmidhuber, "Applying LSTM to time series predictable through time-window approaches," in *Proc. Int. Conf. Artif. Neural Netw.*, 2001, pp. 669–676.

[11] S. Hochreiter and J. Schmidhuber, "Long short-term memory," *Neural Comput.*, vol. 9, no. 8, pp. 1735–1780, Nov. 1997.

[12] M. H. Beale, M. T. Hagan, and H. B. Demuth. (2020). *Deep Learning Toolbox: User's Guide*. [Online]. Available: https://dokumen.pub/MATLAB-deep-learning-toolbox-users-guide-r2020anbsped.html

[13] M. Schuster and K. K. Paliwal, "Bidirectional recurrent neural networks," *IEEE Trans. Signal Process.*, vol. 45, no. 11, pp. 2673–2681, Nov. 1997.

[14] H. Shi, L. Guo, S. Tan, and X. Bai, "Rolling bearing initial fault detection using long short-term memory recurrent network," *IEEE Access*, vol. 7, pp. 171559–171569, 2019.

[15] K. Kuru, "Conceptualisation of human-on-the-loop haptic teleoperation with fully autonomous self-driving vehicles in the urban environment," *IEEE Open J. Intell. Transp. Syst.*, vol. 2, pp. 448–469, 2021.

[16] A. G. B. Richard and S. Sutton, *Reinforcement Learning*. London, U.K.: MIT Press, 2015.

[17] M. B. A. Nandy, *Reinforcement Learning*. Cham, Switzerland: Springer, 2018.

[18] IEC. (1999). *International Standards: Ultrasonics—Flow Measurement Systems—Flow Test Object*. [Online]. Available: https://webstore.iec.ch/preview/info_iec61685%7Bed1.0%7Den.pdf

[19] A. Rabell Montiel, J. E. Browne, S. D. Pye, T. A. Anderson, and C. M. Moran, "Broadband acoustic measurement of an agar-based tissue-mimicking-material: A longitudinal study," *Ultrasound Med. Biol.*, vol. 43, no. 7, pp. 1494–1505, Jul. 2017.

[20] S. Inglis, K. V. Ramnarine, J. N. Plevris, and W. N. McDicken, "An anthropomorphic tissue-mimicking phantom of the oesophagus for endoscopic ultrasound," *Ultrasound Med. Biol.*, vol. 32, no. 2, pp. 249–259, Feb. 2006.

[21] J. A. Zagzebski, *Essentials of Ultrasound Physics*. St. Louis, MI, USA: Mosby, 1996.

[22] J. Berman and H. Abramson, "Effectiveness of psychological and pharmacological treatments for nocturnal enuresis," *J. Consulting Clin. Psychol.*, vol. 62, pp. 737–745, Jan. 1994.

[23] W. I. Forsythe and R. J. Butler, "Fifty years of enuretic alarms," *Arch. Disease Childhood*, vol. 64, no. 6, pp. 879–885, Jun. 1989.

[24] J. Evans, B. Malmsten, A. Maddocks, H. S. Popli, and H. Lottmann, "Randomized comparison of long-term desmopressin and alarm treatment for bedwetting," *J. Pediatric Urol.*, vol. 7, no. 1, pp. 21–29, Feb. 2011.

[25] E. Apos et al., "Enuresis management in children: Retrospective clinical audit of 2861 cases treated with practitioner-assisted bell-and-pad alarm," *J. Pediatrics*, vol. 193, pp. 211–216, Feb. 2018.

• • •